

# $^{16}\text{O} + ^{16}\text{O}$ nature of the superdeformed band of $^{32}\text{S}$ and the evolution of the molecular structure

Masaaki Kimura

*RI-beam Science Laboratory, RIKEN (The Institute of Physical and Chemical Research), Wako, Saitama 351-0198, Japan*

Hisashi Horiuchi

*Department of Physics, Kyoto University, Kitashirakawa, Kyoto 606-8502, Japan*

The relation between the superdeformed band of  $^{32}\text{S}$  and  $^{16}\text{O} + ^{16}\text{O}$  molecular bands is studied by the deformed-base antisymmetrized molecular dynamics with the Gogny D1S force. It is found that the obtained superdeformed band members of  $^{32}\text{S}$  have considerable amount of the  $^{16}\text{O} + ^{16}\text{O}$  component. Above the superdeformed band, we have obtained two excited rotational bands which have more prominent character of the  $^{16}\text{O} + ^{16}\text{O}$  molecular band. These three rotational bands are regarded as a series of  $^{16}\text{O} + ^{16}\text{O}$  molecular bands which were predicted by using the unique  $^{16}\text{O} - ^{16}\text{O}$  optical potential. As the excitation energy and principal quantum number of the relative motion increase, the  $^{16}\text{O} + ^{16}\text{O}$  cluster structure becomes more prominent but at the same time, the band members are fragmented into several states.

PACS numbers: Valid PACS appear here

The properties of the  $^{16}\text{O} + ^{16}\text{O}$  molecular bands have been studied by many authors with the microscopic cluster models for many years [1]. Despite of these studies, the microscopic models have not been able to give a conclusive answer. One of the reasons is the fact that the number of the molecular band, the excitation energy of the band head, and the moment of the inertia strongly depend on the effective nuclear force. Recently, a rather conclusive answer was given by the studies with the macroscopic model [2, 3]. In those studies, the authors used the unique optical potential for the  $^{16}\text{O} - ^{16}\text{O}$  system which was determined in 1990's [4] after the first discovery of the nuclear rainbow in 1989 [5]. These studies gave the following answers for the lowest three rotational bands whose principal quantum numbers  $N=2n+L$  of the relative motion between clusters are  $N=24, 26$  and  $28$ , respectively: The lowest Pauli-allowed rotational band ( $N=24$ ) starts from the  $0^+$  state located at about 9 MeV in the excitation energy (about 8 MeV below the  $^{16}\text{O} + ^{16}\text{O}$  threshold), and the energy gap between the  $N=24$  and  $N=26$  bands and that between  $N=26$  and  $N=28$  bands are both approximately 10 MeV. In Ref.[2], it is proposed that the observed  $^{16}\text{O} + ^{16}\text{O}$  molecular states correspond to the third band whose principal quantum number is  $N=28$ .

Besides the cluster models, in these days, the superdeformed structure of  $^{32}\text{S}$  has been studied by many authors with the mean-field theories [6, 7, 8]. It is largely because the superdeformed structure of  $^{32}\text{S}$  is regarded as a key to understand the relation between the superdeformed state and the molecular structure. Indeed, by the HF(B) calculations, it is shown that the superdeformed minimum of the energy surface is well established in each angular momentum, and at the superdeformed local minimum, the wave function shows the two-center-like character. It is also notable that many of the mean-field calculations

predict that the superdeformed band starts from the  $0^+$  located at around 10 MeV which agrees with the band head energy of the  $N=24$  band obtained from the unique optical potential. Therefore, it is enough conceivable that the superdeformed band obtained by the mean-field calculations and the lowest Pauli-allowed  $^{16}\text{O} + ^{16}\text{O}$  molecular band ( $N=24$ ) are identical.

In the present study, we aim at clarifying the relation between the superdeformed state and the  $^{16}\text{O} + ^{16}\text{O}$  molecular structure. The objectives of the present study are summarized as follows. (1) To what extent the superdeformed state and the  $^{16}\text{O} + ^{16}\text{O}$  molecular structure are related? : In the unique optical potential analysis, the factors which distort the  $^{16}\text{O} + ^{16}\text{O}$  cluster structure such as the effects of the spin-orbit force and the formation of the deformed one-body field are not treated directly. Instead, these factors are renormalized into the optical potential through the extrapolation to the low-energy region. When one treats these factors veraciously by the microscopic models, the pure  $^{16}\text{O} + ^{16}\text{O}$  cluster structure will be distorted and will have a deformed one-body field character. In other words, the superdeformed states in the mean-field models and the states of the lowest Pauli-allowed  $^{16}\text{O} + ^{16}\text{O}$  band of the unique optical potential will be the states which have both characters of the deformed one-body field structure and two cluster structure. Therefore, it will be important to study to what extent each state has the  $^{16}\text{O} + ^{16}\text{O}$  character and the deformed one-body field character. (2) Do the excited states exist in which the excitation energy is spent to excite the relative motion between the clusters? Do they correspond to the  $N=26$  and  $28$  bands obtained from the unique optical potential? : When we believe that the superdeformed states of  $^{32}\text{S}$  have the considerable  $^{16}\text{O} + ^{16}\text{O}$  component, we can expect the excitation mode in which the excitation energy is used to excite the relative motion

between the clusters.

The deformed-base antisymmetrized molecular dynamics (deformed-base AMD) [9] combined with the generator coordinate method (GCM) has been used with the Gogny D1S force [10]. For the sake of the selfcontainedness, we briefly explain this framework. For more details, the reader is referred to the references [11]. The intrinsic basis wave function of the system  $\Phi_{int}$  is expressed by a Slater determinant of single-particle wave packets  $\varphi_i$ . Each single-particle wave packet is composed of spatial part  $\phi_i$ , spin part  $\chi_i$  and isospin part  $\tau_i$ . The spatial part has the form of the deformed Gaussian centered at  $\mathbf{Z}_i$ .

$$\Phi_{int} = \frac{1}{\sqrt{A!}} \det \{ \varphi_i(\mathbf{r}_j) \}, \quad (1)$$

$$\varphi_i(\mathbf{r}_j) = \phi_i(\mathbf{r}_j) \chi_i \tau_i, \quad (2)$$

$$\phi_i(\mathbf{r}) = \exp \{ -\nu_x (x - Z_{ix})^2 - \nu_y (y - Z_{iy})^2 - \nu_z (z - Z_{iz})^2 \}, \quad (3)$$

$$\chi_i = \alpha_i \chi_{i\uparrow} + \beta_i \chi_{i\downarrow}, \quad \tau_i = \text{proton or neutron}. \quad (4)$$

Here, the centroids of the Gaussian  $\mathbf{Z}_i$  and the spin direction  $\alpha_i$  and  $\beta_i$  are complex parameters and are dependent on each particle. The width parameters  $\nu_x$ ,  $\nu_y$  and  $\nu_z$  are common to all particles. These variational parameters ( $Z_i$ ,  $\alpha_i$ ,  $\beta_i$  and  $(\nu_x, \nu_y, \nu_z)$ ) are determined by the variational calculation. The variational calculation is made after the parity projection by using parity-projected wave function  $\Phi^\pi = \frac{1 \pm P_x}{2} \Phi_{int}$  as the variational wave function. In this study, the variational calculation is made under the constraint on the nuclear deformation parameter  $\beta$ . The advantage of the deformed Gaussian basis as the single-particle wave packet is that it is possible to describe both the deformed one-body-field structure and the cluster structure as well as their mixed structure within the same framework. We can confirm this feature when we consider the two limits of the nuclear structure described by this wave function, the deformed-harmonic-oscillator limit and the cluster limit. The deformed-harmonic-oscillator limit is reached when the centroids of all single-particle wave packets ( $\text{Re } \mathbf{Z}_i$ ) are at the center of the nucleus and the single-particle wave packets are deformed. On the contrary, the cluster limit is obtained when the centroids of the single-particle wave packets are separated into the centers of the constituent clusters and the single-particle wave packets are spherical.

After the constrained variational calculation for  $\Phi^\pi$ , we superpose the optimized wave functions for various deformation parameters (GCM):

$$\Phi^{J^\pi} = c P_{MK}^J \Phi^\pi(\beta_0) + c' P_{MK'}^J \Phi^\pi(\beta'_0) + \dots, \quad (5)$$

where  $\Phi^\pi(\beta_0)$  is the optimized wave function under the constraint of the nuclear deformation parameter  $\beta = \beta_0$  and  $P_{MK}^J$  is the angular momentum projector. The coefficients  $c, c', \dots$  are determined by the diagonalization

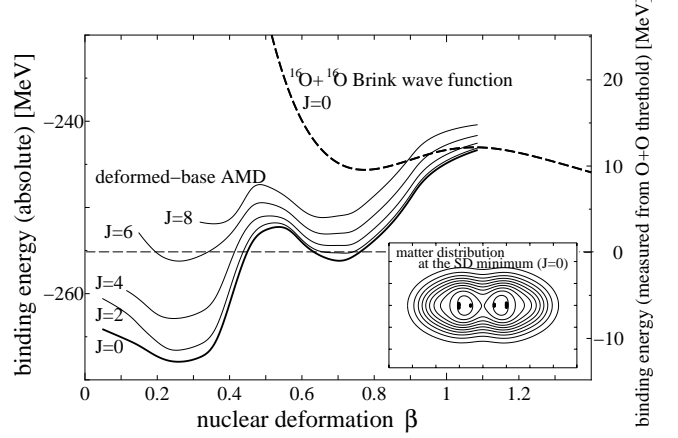


FIG. 1: The energy surface as a function of the nuclear deformation  $\beta$  for  $^{32}\text{S}$ . Dashed curve is for the  $J = 0$  state obtained by the  $^{16}\text{O} + ^{16}\text{O}$  Brink wave function. Solid curves are for  $J = 0, 2, 4, 6$  and  $8$  states obtained by the deformed-base AMD. The matter density distribution of the deformed-base AMD wave function at the superdeformed minimum ( $J=0$ ) is also shown. Small black circles in the density distribution represent the centroids of the single-particle wave packets  $\text{Re } \mathbf{Z}_i$

of the Hamiltonian. When the intrinsic wave function  $\Phi^\pi(\beta_0)$  has a prominent cluster structure, the superposition of the wave functions will improve mainly the description of the relative wave function between clusters, while it will improve mainly the description of the mean-field and other correlations when  $\Phi^\pi(\beta_0)$  has a prominent mean-field character.

Below we explain how we estimate the amount of the  $^{16}\text{O} + ^{16}\text{O}$  component in the obtained wave function  $\Phi^{J^\pi}$ . We rewrite the  $\Phi^{J^\pi}$  by decomposing it into the  $^{16}\text{O} + ^{16}\text{O}$  component and the residual part,

$$\Phi^{J^\pi} = \alpha \mathcal{A} \{ \chi_J(r) Y_{J0}(\hat{r}) \phi(^{16}\text{O}) \phi(^{16}\text{O}) \} + \sqrt{1 - \alpha^2} \Phi_r, \quad (6)$$

where  $\mathcal{A}$  is the antisymmetrizer,  $\mathbf{r}$  is the relative coordinate between two  $^{16}\text{O}$  clusters and  $\phi(^{16}\text{O})$  is the internal wave function of the  $^{16}\text{O}$  cluster.  $\chi_J(r)$  is so normalized that  $\mathcal{A} \{ \chi_J(r) Y_{J0}(\hat{r}) \phi(^{16}\text{O}) \phi(^{16}\text{O}) \}$  is normalized to unity.  $\Phi_r$  is orthogonal to the  $^{16}\text{O} + ^{16}\text{O}$  cluster space. It is possible to evaluate the amount of the  $^{16}\text{O} + ^{16}\text{O}$  component  $w^J = |\alpha|^2 = |\langle \Phi^{J^\pi} | P_L^J | \Phi^{J^\pi} \rangle|^2$  with the projection operator  $P_L^J = \sum_\alpha |\tilde{\varphi}_\alpha^J\rangle \langle \tilde{\varphi}_\alpha^J|$  onto the  $^{16}\text{O} + ^{16}\text{O}$  cluster model space, where  $\tilde{\varphi}_\alpha^J$  is the orthonormalized set of the spin projected Brink wave functions for  $^{16}\text{O} + ^{16}\text{O}$  system. In this study, 26 spin-projected Brink wave functions with the inter-cluster distance ranging from 0.5 fm to 13.0 fm are orthonormalized to construct  $\tilde{\varphi}_\alpha^J$ .

Before discussing the results of the deformed-base AMD+GCM, we show the result of the calculation in which we use the intrinsic wave functions which have the pure  $^{16}\text{O} + ^{16}\text{O}$  configuration. The Brink wave function is used for the intrinsic  $^{16}\text{O} + ^{16}\text{O}$  wave function. Therefore, this result is the same as the traditional cluster

model calculation of  $^{16}\text{O}+^{16}\text{O}$  RGM (resonating group method) and  $^{16}\text{O}+^{16}\text{O}$  GCM. In Fig. 1, the energy surface for the  $J = 0$  state as a function of the nuclear deformation is shown (dashed curve). We note that the  $^{16}\text{O}+^{16}\text{O}$  configuration describes more than  $4\hbar\omega$  excited states relative to the ground state of  $^{32}\text{S}$ , therefore the ground state and the normal deformed states are not included in this energy surface. It has the energy minimum at  $\beta = 0.73$  (inter-cluster distance is 5.0 fm) which corresponds to two touching  $^{16}\text{O}$ . The minimum energy is about 8 MeV higher than the  $^{16}\text{O}+^{16}\text{O}$  threshold energy. After the GCM calculation along this energy surface, we have obtained three rotational bands which have the quantum numbers of the relative motion  $N=24, 26$  and  $28$ , respectively, and are shown by dashed lines in FIG. 2. However, their energies are too high to coincide with the rotational bands obtained from the unique optical potential and also with the superdeformed band obtained from the HF(B) calculations. The energy gaps between these bands (4 MeV between  $N=24$  and  $N=26$ , and 6 MeV between  $N=26$  and  $N=28$  in the case of  $0^+$  states) are much smaller than the results from the unique optical potential. We think that these deviations come from the fact that the effects which distort the cluster structure are neglected in the Brink wave function. We will see below that in fact the effects of the distortion are fairly large.

In Fig. 1, the energy surfaces for  $J = 0$  to  $J = 8$  states obtained by the deformed-base AMD+GCM calculation are also shown. Since the AMD wave function does not assume any cluster configuration, the normal deformed states also appear in these energy surfaces. In the normal deformed states, the prolate deformed states and the triaxially deformed states ( $\gamma = 6^\circ \sim 30^\circ$ ) are energetically degenerate. After the GCM calculation, prolate wave functions mainly contribute to the ground band while the triaxially deformed wave functions to the first excited band. Their excitation energies and the intraband  $E2$  transition probabilities (Table I) show reasonable agreement with experiments and are consistent with the results of the HFB calculation with the Gogny D1S force [8], though the total binding energy of the ground state underestimates the experimental data by about 2.0 MeV.

We also find that the behavior of the energy surface around the excited local minimum is similar to that of the HF(B) calculations. In each angular momentum state, the superdeformed minimum is well developed and the  $0^+$  excitation energy relative to the normal deformed ground state is around 10 MeV. The energy difference between the deformed-base AMD and the  $^{16}\text{O}+^{16}\text{O}$  calculation at the superdeformed minimum is about 10 MeV, which implies a fairly large effect of the distortion of the cluster structure. Indeed, the deformed-base AMD wave function deviates from the pure cluster limit. At the superdeformed limit, the single-particle wave pack-

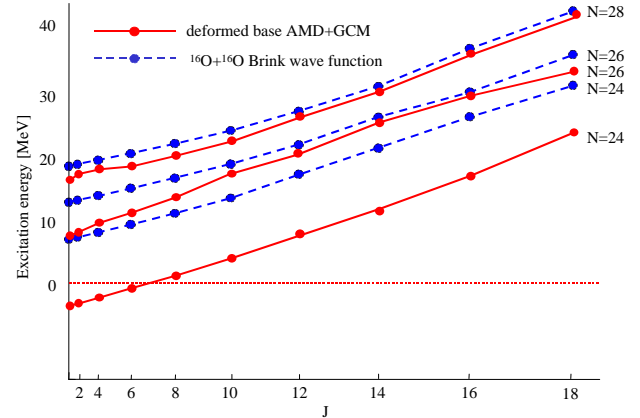


FIG. 2: The excitation energies of the  $N=24, 26$  and  $28$  band members obtained by the  $^{16}\text{O}+^{16}\text{O}$  Brink wave function (dashed lines) and the deformed-base AMD+GCM (solid lines). The  $N=26$  and  $N=28$  band members are fragmented into several states in the deformed-base AMD+GCM calculation and the averaged energies  $E_{AV}$  are shown for these bands.

ets are prolate deformed ( $\nu_x = \nu_y = 0.160 \text{ fm}^{-2}$  and  $\nu_z = 0.115 \text{ fm}^{-2}$ ), and the distance between the centroids of the single-particle wave packets are rather small (3.1 fm), though they are separated into two parts (centers of two  $^{16}\text{O}$ ) and show two-center nature. The energy gain by the deformed-base AMD function compared to the pure  $^{16}\text{O}+^{16}\text{O}$  wave function mainly comes from the two-body spin-orbit force and the density dependent force. In the case of the deformed-base AMD wave function, the expectation value of the two-body spin-orbit force is about -4.5 MeV which must be zero in the pure  $^{16}\text{O}+^{16}\text{O}$  wave function. Though its value is not so large, it lowers the excitation energy of the superdeformed state from the  $^{16}\text{O}+^{16}\text{O}$  limit. Compared to the  $^{16}\text{O}+^{16}\text{O}$  wave function, the expectation value of the repulsive density dependent force is about 6 MeV smaller in the deformed-base AMD wave function and it also indicates the non-small deviation from the  $^{16}\text{O}+^{16}\text{O}$  structure. Though the kinetic energy does not much contribute to lower the energy of the superdeformed band, its nature is different from the case of the pure  $^{16}\text{O}+^{16}\text{O}$  structure. At the superdeformed minimum, the single-particle wave packets are prolate deformed and since the kinetic energy is almost linear to width parameter  $\nu$ , the kinetic energy to the  $z$  direction is eased. However, we have found that the wave function of the deformed-base AMD (which is parity and the angular momentum projected) at the superdeformed minimum still has a considerable amount of the  $^{16}\text{O}+^{16}\text{O}$  component,  $w^{J=0} = 0.57$ .

After the GCM calculation by superposing the deformed-base AMD wave functions along the energy surface, we have obtained three rotational bands. The low-

TABLE I: Excitation energy  $Ex$  [MeV] and the intra-band  $E2$  transition probabilities  $B(E2; J \rightarrow J-2)$  [ $e^2 \text{fm}^4$ ] of the ground band and the first excited band.

$J$	ground (Theor)		ground (Exp)		band I (Theor)		band I (Exp)	
	$Ex$	$B(E2)$	$Ex$	$B(E2)$	$Ex$	$B(E2)$	$Ex$	$B(E2)$
0	-	-	-	-	3.9	-	3.778	-
2	2.3	66	2.23	$60 \pm 6$	4.8	31	4.282	-
4	5.75	109	4.459	$72 \pm 12$	10.1	88	6.852	$35.4^{+18.6}_{-8.4}$
6	10.2	130	8.346	$> 22.2$	12.9	98	9.783	-

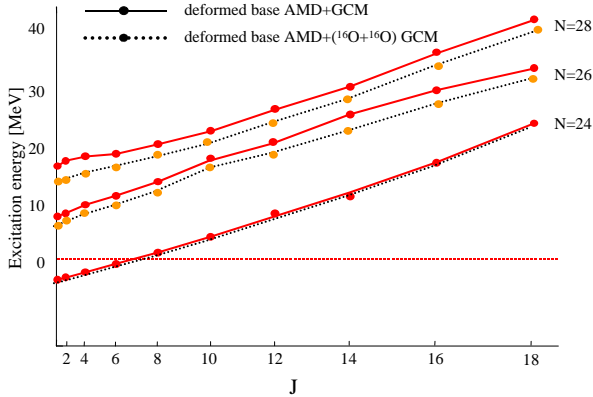


FIG. 3: The excitation energies of the  $N=24$ ,  $26$  and  $28$  band members obtained by the deformed-base AMD+GCM (solid lines) and the deformed-base AMD+ $(^{16}\text{O}+^{16}\text{O})$ +GCM (dotted lines). The  $N=26$  and  $N=28$  band members are fragmented into several states in both calculations and the averaged energies  $E_{\text{AV}}$  are shown for these bands. The deformed-base AMD+GCM results in this figure are the same as those of FIG. 2.

est superdeformed band, the second lowest band and the third band have large  $^{16}\text{O}+^{16}\text{O}$  components with  $N=24$ ,  $26$  and  $28$ , respectively. Thus these three bands correspond to the  $N=24$ ,  $26$  and  $28$  bands of the unique optical potential. We refer to these bands simply as  $N=24$ ,  $26$  and  $28$  bands (Fig. 2). The band members of the  $N=26$  and  $28$  bands are fragmented into several states. Namely, there are several states which have the  $^{16}\text{O}+^{16}\text{O}$  component of the same principal quantum number  $N$ . For example, the  $0^+$  state of the  $N=26$  band is fragmented into three states in which  $w^{J=0}$  are  $0.34$ ,  $0.13$ , and  $0.25$ , respectively. In the following, we only show the averaged energies of these fragmented states to investigate the gross feature of the band structure and the fragmentation is discussed later. The averaged energy is calculated by multiplying the overlap  $w_i$  as the weight;  $E_{\text{AV}}^J = (w_1^J E_1^J + w_2^J E_2^J + \dots) / (w_1^J + w_2^J + \dots)$ . The excitation energies of the  $N=24$  band members are lowered by about 3 MeV compared to those of the band formed by the states at the superdeformed energy minimums.

This may be due to the improvement of the description of the mean-field and the collective motion by the GCM calculation, since in the  $N=24$  band, the amount of the  $^{16}\text{O}+^{16}\text{O}$  component is decreased by the GCM calculation;  $w^{J=0} = 0.57$  for the deformed-base AMD wave function and  $w^{J=0} = 0.42$  for the deformed-base AMD+GCM wave function. It is important that the energy gain of the deformed-base AMD+GCM band compared to the pure  $^{16}\text{O}+^{16}\text{O}$  band becomes smaller as the excitation energy of the relative motion between clusters becomes larger. For example, compared to the pure  $^{16}\text{O}+^{16}\text{O}$  bands, the  $0^+$  states of  $N=24$ ,  $26$  and  $28$  bands are lowered by about 12, 6 and 2 MeV, respectively. This decrease of the energy gain means the enhancement of the  $^{16}\text{O}+^{16}\text{O}$  molecular structure in the higher excited bands. Indeed, the sum of the  $w^J$  of the fragmented band members drastically increases in  $N=26$  and  $28$  bands compared to that of the  $N=24$  band; they amount to 0.71 and 0.73 for the case of the  $0^+$  states of the  $N=26$  and  $28$  bands.

In the framework of the deformed-base AMD+GCM, the basis states for the GCM calculation are obtained from the variational calculation. Since the variational calculation optimizes mainly the lowest  $N=24$  band members in which the  $^{16}\text{O}+^{16}\text{O}$  molecular structure is distorted, these basis states may be inappropriate to describe the  $N=26$  and  $N=28$  bands in which the  $^{16}\text{O}+^{16}\text{O}$  molecular structure is drastically enhanced. In other words, the present calculation may underestimate the enhancement of the  $^{16}\text{O}+^{16}\text{O}$  molecular structure in  $N=26$  and  $N=28$  bands. Therefore, we have included the  $^{16}\text{O}+^{16}\text{O}$  Brink wave functions in the basis states of the GCM calculation in addition to the deformed-base AMD wave functions obtained from the variational calculation. The obtained results of the enlarged GCM calculation are shown in Fig. 3. The enhancement of the  $^{16}\text{O}+^{16}\text{O}$  molecular structure has become more prominent in  $N=26$  and  $N=28$  bands. It is reasonable that the excitation energies and the overlaps  $w^J$  of the  $N=24$  band members do not change much, since in this band, the  $^{16}\text{O}+^{16}\text{O}$  molecular structure is distorted and the inclusion of the pure  $^{16}\text{O}+^{16}\text{O}$  configuration is less important. On the contrary, in the  $N=26$  and  $28$  bands, the excitation energies are lowered by about a few MeV and the amounts of the  $^{16}\text{O}+^{16}\text{O}$  component have increased drastically. The sums of the fragmented  $w^J$  for  $N=26$  and

TABLE II: The excitation energies  $E_x$  and the amounts  $w^J$  of the  $^{16}\text{O}+^{16}\text{O}$  components of the fragmented  $0^+$  states of  $N=26$  and 28 bands.

	N=26		N=28	
	$E_x$	$w^J$	$E_x$	$w^J$
fragment I	23.8	0.54	31.2	0.32
fragment II	24.0	0.13	34.0	0.45
fragment III	25.3	0.23	38.7	0.20
$E_{\text{AV}}$ and $\sum w^J$	24.2	0.90	33.7	0.98

28 bands are 0.90 and 0.98, respectively. It is interesting that the highest N=28 band members have almost pure  $^{16}\text{O}+^{16}\text{O}$  molecular structure when we sum up the fragmented states, and it looks plausible that these band members are assigned to correspond to the observed molecular resonances of  $^{16}\text{O}+^{16}\text{O}$  as is proposed in Ref.[2].

Finally, we discuss the fragmentation of the N=26 and 28 band members. The judgement whether a fragment belongs to the N=26 or 28 band is determined by evaluating the amount of the overlaps with the N=26 and 28 band members obtained from the GCM calculation with the pure  $^{16}\text{O}+^{16}\text{O}$  wave function. As an example, the energies and the amounts of the  $^{16}\text{O}+^{16}\text{O}$  component for  $0^+$  fragments are listed in Table II. The  $0^+$  states of the N=26 and 28 bands are fragmented into three states. In the present calculation, the number of the fragments do not strongly depend on the angular momentum and the principal quantum number N. At most, the  $12^+$  state of N=28 band is fragmented into five states. These fragmentations are mainly caused by the coupling with the states with medium deformation which appear as a small peak between normal deformed states and the superdeformed states and also by the coupling with the  $^{16}\text{O}+^{16}\text{O}^*$  states which are included in the largely deformed ( $\beta > 0.9$ ) wave functions where  $^{16}\text{O}^*$  stands for distorted  $^{16}\text{O}^*$  cluster. Details of these couplings are important to compare the present results and the experiments and will be investigated in the future.

To summarize, we have shown that the superdeformed band obtained from the HF(B) calculations and the Pauli-allowed lowest N=24 band of the  $^{16}\text{O}+^{16}\text{O}$  molecular bands are essentially identical. In this band,  $^{16}\text{O}+^{16}\text{O}$  molecular structure is distorted by the effects of the deformed mean-field formation and the spin-orbit force. This distortion is not small and lowers the excitation energy largely, but this band members still have the consid-

erable component of the  $^{16}\text{O}+^{16}\text{O}$  molecular structure. We have obtained two excited bands which are generated by the excitation of the relative motion between two  $^{16}\text{O}$  clusters contained in the  $^{16}\text{O}+^{16}\text{O}$  component of the superdeformed band. In the excited N=26 and 28 bands, the distortion is less important and the band members have the prominent molecular structure. The members of these bands are fragmented into several states and the assignment of the N=28 band members to the observed  $^{16}\text{O}+^{16}\text{O}$  molecular resonances looks plausible.

The authors would like to thank Dr. Y. Kanada-En'yo for useful discussions. Most of the computational calculations were carried out by SX-5 at Reserch Center for Nuclear Physics, Osaka University (RCNP). This work was partially performed in the gResearch Project for Study of Unstable Nuclei from Nuclear Cluster Aspects sponsored by Institute of Physical and Chemical Research (RIKEN).

---

[1] For example, H. Friedrich, Nucl. Phys. **A224**, 537 (1974).  
D. Baye et al., Nucl. Phys. **A258**, 157 (1976); **A276**, 354 (1977).  
T. Ando, A. Tohsaki and K. Ikeda, Prog. Theor. Phys. **61**, 101 (1979); **64**, 1608 (1980).

[2] S. Ohkubo and K. Yamashita, Phys. Rev. **C 66**, 021301(R) (2002).

[3] Y. Kondō, B. A. Robson and R. Smith, Proceedings of the Fifth International Conference on Cluster Aspects in Nuclear and Subnuclear Systems, Kyoto, Japan, 597, (K. Ikeda et al., Physical Society of Japan, 1988)

[4] M.P. Nicoli, Ph.D. thesis, Strasbourg, 1998.  
W. von Oertzen, H.G. Bohlen and D. T. Khoa, Proceedings of the International Symposium on Physics of Unstable Nuclei, Halong Bay, Vietnam, 202c, (D. T. Khoa et al., North-Holland, 2002).

[5] E.Stiliaris et al., Phys. Lett. **B223**, 291 (1989).

[6] M. Yamagami and K. Matsuyanagi, Nucl. Phys. **A672**, 123 (2000).

[7] H. Molique, J. Dobaczewski, and J. Dudek1, Phys. Rev. **C 61**, 044304 (2000) .

[8] R. R. Rodríguez-Guzmán, J. L. Egido, and L. M. Robledo, Phys. Rev. **C 62**, 054308 (2000).

[9] M. Kimura, submitted to Phys. Rev. C.

[10] J. Decharge and D. Gogny, Phys. Rev. **C 21**, 1568 (1980).

[11] For example, Y. Kanada-En'yo and H. Horiuchi, Phys. Rev. **C 52**, 647 (1995).